[15] Biber K, Lubrich B, Fiebich BL, Boddeke H, van Calker D. Interleukin-6 enhances expression of adenosine A1 receptor mRNA and signaling in cultured rat cortical astrocytes and brain slices. Neuropsychopharmacology 2001;24:86–96.
[16] Dragnow M. Adenosine and seizure termination. Ann Neurol 1991;29:575.
[17] Luca GD, Di Giorgio RM, Macaione S, Calpona PR, Costantino S, Di Paola ED, et al. Susceptibility to audiogenic seizures and neurotransmitter amino acid levels in different brain areas of IL-6-deficient mice. Pharmacol Biochem Behav 2004;78: 75–81.
[18] De Sarro G, Russo E, Ferrei G, Giuseppe B, Flocco MA, Di Paola ED, et al. Seizure susceptibility to various convulsant stimuli of knockout interleukin-6 mice. Pharmacol Biochem Behav 2004;77:761–6.
[19] Ray A, Gulati K, Anand S, Vijayan VK. Pharmacological studies on mechanisms of aminophylline-induced seizures in rats. Indian J Exp Biol 2005;43:849–53.
[20] Odajima Y, Nakano H, Kato T. Clinical review on patients who developed seizures during theophylline administration: relationships with seizure-predisposing factors (in Japanese). Arerugi (Tokyo) 2006;55:1295–303.

Eur J Pediatr
DOI 10.1007/s00431-007-0607-8

SHORT REPORT

Partial hypoxanthine-guanine phosphoribosyltransferase deficiency due to a newly recognized mutation presenting with renal failure in a one-year-old boy

Yasushi Ishida · Asako Ishimaru · Hisamichi Tauchi · Akiko Yamaguchi · Masayoshi Yokoyama · Kazuhiro Hiroi · Nobuaki Wakamatsu · Yasukazu Yamada

Received: 26 March 2007 / Accepted: 1 September 2007

Abstract We describe the case of a 1-year-old boy with partial hypoxanthine-guanine phosphoribosyltransferase (HPRT) deficiency. At his first visit to the hospital, he was diagnosed with hyperuricemia and irreversible renal failure. The misssense mutation Asp185Gly (554A>G) was identified in exon 8 of his HPRT gene, and this mutation was inherited from the mother.

Keywords Renal failure · Partial HPRT deficiency · HPRT gene · Hyperuricemia · New mutation

Abbreviations

HPRT	hypoxanthine-guanine phosphoribosyltransferase
APRT	adenine phosphoribosyltransferase
PCR	polymerase chain reaction

Y. Ishida (✉) · A. Ishimaru · H. Tauchi
Department of Pediatrics,
Ehime University Graduate School of Medicine,
Touon-City, Ehime 791-0295, Japan
e-mail: ishida@m.ehime-u.ac.jp

A. Yamaguchi · M. Yokoyama
Department of Urology,
Ehime University Graduate School of Medicine,
Ehime, Japan

K. Hiroi
Division of Pediatrics, Yawatahama-City Hospital,
Ehime, Japan

N. Wakamatsu · Y. Yamada
Department of Genetics, Institute for Developmental Research,
Aichi Human Service Center,
Aichi, Japan

Hypoxanthine-guanine phosphoribosyltransferase (HPRT, OMIM 308000) is a purine salvage enzyme that converts the purine bases hypoxanthine and guanine to their respective mononucleotides using phosphoribosyl-l-pyrophosphate. HPRT deficiency is an inherited disorder, and it develops due to a defect in the HPRT gene, which is located on the long arm of the X-chromosome (Xq26-q27) [3]. The aim of this report is to present the case of a 1-year-old patient with partial HPRT deficiency (without neurological or behavioral abnormalities) suffering from renal failure and to describe a newly recognized point mutation detected in his HPRT gene.

Patient report

A one-year-old boy was referred to our hospital because of bad temper, fever, tachypnea, and passage of renal stones. He was the only child of nonconsanguineous parents (33-year-old father and 23-year-old mother). The infant had no prenatal or birth problems, but he suffered from failure to thrive since 6 months of age. On admission, physical examination revealed that the toddler was drowsy and inactive with tachypnea (55/min) and a pale face. His height was 70.4 cm (−2.4 SD), his weight was 6.9 kg (−2.7 SD), blood pressure was 114/54 mmHg, body temperature was 38.2 C, pulse rate was 180/min, and neurological evaluations were normal. There was no evidence of gouty arthritis.

He presented with prominent acidosis (pH, 7.089; BE, −25.6 mmol/l) caused by renal failure (BUN, 84 mg/dl; creatinine, 2.1 mg/dl) and hyperuricemia (25.3 mg/dl) with renal stones, but there were no signs of gout or

neurological and behavioral abnormalities. Complete blood cell count revealed mild anemia. Urinalysis showed moderate hematuria and proteinuria in diluted urine (<1,005). The clearance of uric acid (C_{UA}) was 5.16 ml/min and that of creatinine (C_{Cr}) was 17.1 ml/min. The uric acid excretion ratio (C_{UA}/C_{Cr}) was 30% (normal, 4–14%). Renal CT showed one small calculus in each kidney.

The patient was treated with continuous ambulatory peritoneal dialysis, allopurinol, adequate hydration with urinary alkalization, and erythropoietin. Due to these treatments, the serum and the urine uric acid levels were restored to normal. After a 24-month follow-up, his physical was found to be normal at the age of 3 years with height of 88.5 cm (−1.2 SD), body weight of 12.8 kg (−0.5 SD), head circumference of 47.3 cm (−1.5SD), and his neuropsychological status developmental score was 106.

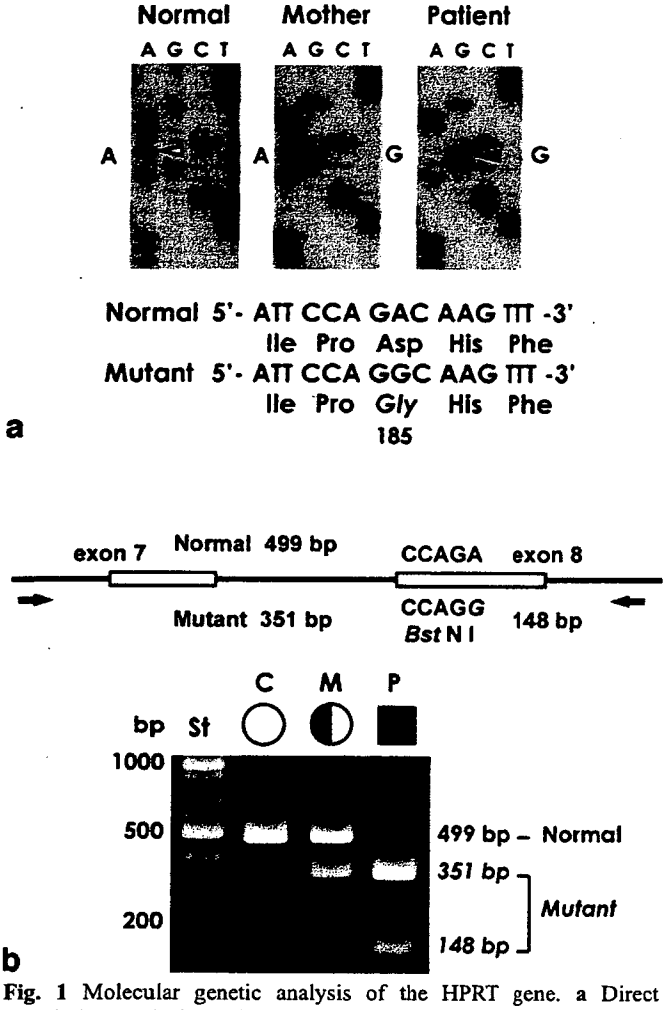

Fig. 1 Molecular genetic analysis of the HPRT gene. **a** Direct sequencing analysis of the DNA fragment including exons 7 and 8. DNA segments containing exons 7 and 8 were amplified from genomic DNA of the patient, his mother, and normal control by PCR described previously. The fragment was sequenced directly by the specific primer (HE8A: 5'-AGA GAG GCA CAT TTG CCA GT-3'). A misssense mutation Asp185Gly (554A>G) in exon 8 of the patient's HPRT gene was identified and his mother was the heterozygous carrier of the mutation showing both A and G bands at the mutation site. **b** Detection of the mutant HPRT gene using PCR-RFLP methods. DNA segments containing exons 7 and 8 were amplified from genomic DNAs of the patient (*P*), his mother (*M*), and normal control (*C*). Utilizing restriction enzyme *Bst* NI the site of CC (A/T)GG was recognized, mutant fragments including the mutation (554A>G) digested to 351 bp and 148 bp were separated from the normal one (499 bp) using 1.5% agarose gel electrophoresis. The mother showed both normal and mutant fragments, indicating a heterozygous carrier

Enzyme activity of RBC

The HPRT activity in the patient's RBC was 0.56± 0.28 nmol/min/mg Hb, which decreased to 30% of that in normal RBC (1.76±0.28 described previously [8]). The HPRT activity in his mother (heterozygous carrier) was normal (1.63±0.07). The adenine phosphoribosyltransferase (APRT) activity in the patient's RBC (0.77±0.08 nmol/min/mg Hb) increased to 1.8 times that in the normal RBC (0.42± 0.10) and that of his mother (0.44±0.02), as is typically described in HPRT deficiency.

Gene analysis

We examined the molecular and genetic basis of the patient's condition according to previously described procedures [8]. By direct sequencing of the fragments, including exon 8, a transition of 554A>G that resulted in a missense mutation of Asp185Gly in the HPRT gene was observed in the patient and his mother who was a heterozygous carrier of the mutation (Fig. 1a). No other abnormalities were detected in the coding exons of HPRT, and the same substitution was found in the reverse transcribed mRNA (cDNA) obtained from the patient (data not shown). The mutation (554A>G) was easy to detect by PCR-RFLP analysis utilizing the *Bst* NI created in the mutant gene (Fig. 1b).

Discussion

To date, more than 300 different HPRT gene mutations have been reported in the Lesch-Nyhan syndrome (OMIM 300322) [4, 5]. A missense mutation of Asp185Gly (554A>G) in exon 8 of the HPRT gene was identified in our patient. The alteration in the patient's enzyme activity (30% of normal) resulted in the overproduction of uric acid,

hyperuricemia, and nephrolithiasis. The patient's mother was heterozygous for the mutation. To the best of our knowledge from previous reports [4, 5] and the database in the website of the Lesch-Nyhan disease international study group (http://www.lesch-nyhan.org/), the identified mutation has not been previously reported, but some mutations in exon 8 associated with partial HPRT deficiency were identified previously.

To the best of our knowledge [1, 2, 6, 7], renal failure has been rarely reported in the case of partial HPRT deficiency during infancy. Infant cases present with failure to thrive, hyperuricemia, and renal insufficiency, which are identical to our patient's symptoms. Partial HPRT deficiency is considered to be rare (one fifth to one tenth of the incidence of Lesch-Nyhan syndrome); however, its renal involvement appeared to be frequent. It is important to increase awareness about partial HPRT deficiency as a cause of renal failure particularly in infants or toddlers because renal failure can be controlled with early allopurinol intervention in most cases.

In conclusion, the prognosis of partial HPRT deficiency in children and adolescents was considered to be good when treated with allopurinol, but renal failure in childhood is one of the life-threatening complications in the case of partial HPRT deficiency.

References

1. Batch JA, Riek RP, Gordon RB, Burke JR, Emmerson BT (1984) Renal failure in infancy due to over-production of urate. Aust N Z J Med 14:852–854
2. Holland PC, Dillon MJ, Pincott J, Simmonds HA, Barratt TM (1983) Hypoxanthine guanine phosphoribosyl transferase deficiency presenting with gout and renal failure in infancy. Arch Dis Child 58:831–833
3. Jinnah H, Friedmann T (2001) Lesch-Nyhan disease and its variants. In: Scriver C (ed) The metabolic and molecular bases of inherited disease, vol 2. McGraw-Hill, New York, pp 2537–2561
4. Jinnah HA, DeGregorio L, Harris JC, Nyhan WL, O'Neill JP (2000) The spectrum of inherited mutations causing HPRT deficiency: 75 new cases and a review of 196 previously reported cases. Mutat Res 463:309–326
5. Jinnah HA, Harris JC, Nyhan WL, O'Neill JP (2004) The spectrum of mutations causing HPRT deficiency: an update. Nucleos Nucleot Nucl 23:1153–1160
6. Lorentz WB Jr, Burton BK, Trillo A, Browning MC (1984) Failure to thrive, hyperuricemia, and renal insufficiency in early infancy secondary to partial hypoxanthine-guanine phosphoribosyl transferase deficiency. J Pediatr 104:94–97
7. Wingen AM, Loffler W, Waldherr R, Scharer K (1985) Acute renal failure in an infant with partial deficiency of hypoxanthine-guanine phosphoribosyltransferase. Proc Eur Dial Transplant Assoc Eur Ren Assoc 21:751–755
8. Yamada Y, Goto H, Suzumori K, Adachi R, Ogasawara N (1992) Molecular analysis of five independent Japanese mutant genes responsible for hypoxanthine guanine phosphoribosyltransferase (HPRT) deficiency. Hum Genet 90:379–384

Silencing of *MYCN* by RNA interference induces growth inhibition, apoptotic activity and cell differentiation in a neuroblastoma cell line with *MYCN* amplification

KEIGO NARA[1], TAKESHI KUSAFUKA[2], AKIHIRO YONEDA[1], TAKAHARU OUE[1], SURASAK SANGKHATHAT[1] and MASAHIRO FUKUZAWA[1]

[1]Department of Pediatric Surgery, Osaka University Graduate School of Medicine, Suita, Osaka 565-0871; [2]Department of Pediatric Surgery, Nihon University School of Medicine, Itabashi, Tokyo 173-8610, Japan

Received November 24, 2006; Accepted January 19, 2007

Abstract. Although it has been suggested that the MYCN oncoprotein functions may influence tumorigenesis and patient survival in neuroblastoma, the mechanism of these functions remains unclear. To elucidate such molecular and biological mechanisms, we performed knock-down of *MYCN* expression using RNA interference (RNAi) method. *MYCN*-siRNAs (*MYCN*-siRNA) were transfected into the *MYCN*-amplified cell line NB-1. To verify the sequence specificity of the siRNA, we prepared three control groups (siRNA control group: siRNAs with no significant homology to any known sequences in human genome, mock control group: reagent and PBS, and the untransfected control group). The cells were analyzed by real-time RT-PCR, Western blotting, immunocytochemistry for gene expression. Cell proliferation activity was measured by WST-1 assay. TUNEL staining was performed to evaluate apoptosis. After the *MYCN*-siRNA transfection, the expression level of the *MYCN* mRNA was significantly reduced to 30% of those of the three control groups ($p<0.05$). Western blotting revealed an obvious reduction in MYCN protein level in the *MYCN*-siRNA group. On immunocytochemistry, intensity of nuclear staining of MYCN was weaker in the *MYCN*-siRNA group than in the three control groups. On WST-1 viability assay, cell proliferation after the *MYCN*-siRNA transfection was significantly suppressed compared to the three control groups ($p<0.05$). The TUNEL positive cells were frequently observed in the *MYCN*-siRNA group. Additionally, after the *MYCN*-siRNA transfection, the morphologic change which was suggestive of neuronal cell differentiation was observed and *TrkA* and *TrkC* expressions were also significantly up-regulated. Using RNAi method, the knock-down of *MYCN* expression induced growth-inhibition, apoptotic activity and cell differentiation in *MYCN*-amplified NB-1 cell line.

Correspondence to: Dr Akihiro Yoneda, Department of Pediatric Surgery, Osaka University Graduate School of Medicine, 2-2 Yamadaoka, Suita, Osaka 565-0871, Japan
E-mail: yoneda@pedsurg.med.osaka-u.ac.jp

Key words: MYCN, neuroblastoma, RNA interference

Introduction

Neuroblastoma (NB), a malignant neoplasm of neural crest origin, is the most common solid extracranial tumor in children and is responsible for 15% of pediatric cancer deaths (1-3). The advent of combination of surgery, chemotherapy and radiation therapy, in addition to high dose chemotherapy with stem cell rescue has made significant improvement in terms of survival rates for advanced NBs. However, the prognosis of the advanced NBs, especially tumors with *MYCN* amplification, remains poor (4,5).

MYCN is one of *MYC* family members which are transcription factors that contain to a transcriptional activation domain and a transcriptional regulation domain (6,7). While *MYCN* expression is limited to early stages of embryonic development, the *MYC* gene is expressed in a wide variety of tissues. *MYCN* is normally located on the distal short arm of chromosome 2, but in cells with *MYCN* amplification it also maps to the double minutes or homogeneously staining regions (8). A large region from chromosome 2p24 (including the *MYCN* locus) becomes amplified, presumably because it provides some selective advantage to the cells (7).

In clinical studies *MYCN* amplification has been correlated with advanced stages of disease and rapid tumor progression (9-11). It is generally accepted that amplification of the *MYCN* oncogene is more relevant to prognosis than other prognostic factors such as chromosome 1p deletion, diploid DNA content and *TrkA* expression. In general, there is a correlation between *MYCN* copy number and expression (11,12). Furthermore, a couple of reports have suggested an association between *MYCN* overexpression and patients' prognosis (12). However, it is still controversial whether or not overexpression of *MYCN* mRNA or MYCN protein has prognostic significance in tumors lacking *MYCN* amplification (13-15).

In an experimental model, it was reported that transgenic mice with overexpression of *MYCN* developed NBs (16). Moreover, Manohar *et al* have shown direct evidence that *MYCN* induction in human NB cells resulted in increased *MRP1* mRNA and protein levels, which in turn was

accompanied by increased drug resistance and enhanced MRP1-mediated drug efflux (17). These studies provide evidence, suggesting that *MYCN* overexpression in NB is a possible biochemical pathway that contributes to the malignant behavior.

A recent discovery of RNA interference (RNAi), as a highly efficient method for gene knock-down, has been one of the major breakthroughs in molecular medicine (18,19). RNAi provides a new reliable method to investigate gene function that has many advantages over other nucleic-acid-based approaches such as antisense oligonucleotides, and which is therefore currently the most widely used gene-silencing technique in functional genomics. The previous extensive research on the development of therapeutic antisense nucleic acids should facilitate development of therapeutic siRNAs (20). Although several recent studies have demonstrated high efficiency and versatility of RNAi in cell cultures, the knock-down of *MYCN* in amplified NB cell line with RNAi has not been reported yet.

In this study, in order to elucidate the role of *MYCN* molecular and biological mechanisms, we transfected artificially synthesized siRNAs that were designed to target the *MYCN* gene by adopting lipofection method as a siRNA delivery system.

Materials and methods

Cell lines and culture condition. *MYCN*-amplified human NB cell line NB-1 was obtained from the Health Science Research Resources Bank (HSRRB, Osaka, Japan). NB-1 cells were propagated and maintained in RPMI-1640 medium (Nacalai tesque, Kyoto, Japan) supplemented with 10% fetal bovine serum (MP Biomedical, Inc., Eschwege, Germany) and anti-biotic-anti-mycotic solution (Nacalai tesque), and cultured in a 37°C humidified atmosphere containing 5% CO_2.

SiRNA oligonucleotides. A cocktail of three siRNA oligo-nucleotides targeting human *MYCN* with two thymidine residues (dTdT) at the 3'-end of the sequence was purchased from B-Bridge International Inc. (Sunnyvale, CA). These siRNA oligonucleotides corresponded to nucleotides 536-554, 1526-1544, and 1654-1672 of the human *MYCN* gene (GeneBank Access no. NM 005378). The sequences are as follows: si*MYCN*-1 (sense 5'-CGGAGATGCTGCTT GAGAA-3'), si*MYCN*-2 (sense 5'-CGGAGTTGGTAAAGA ATGA-3'), si*MYCN*-3 (sense 5'-CAGCAGTTGCTAAAGA AAA-3').

Each siRNA oligonucleotide included in the cocktail was separately available and used for preliminary experiments. To verify sequence specific effectiveness of the *MYCN*-siRNAs, we also used negative control siRNAs (NC-siRNA, B-Bridge International Inc.) that have no significant homology with any known sequences in the human genome.

Transfection. Transient transfection of siRNA was carried out using a commercially available transfection reagent (HiPerFect, Qiagen Inc., Valencia, CA), according to the instruction manual. Transfections were performed with a final concentration of 25 or 50 nM of siRNA in serum-free culture media. In this step, we adopted a reverse transfection method, in which cell seeding and transfection were performed simultaneously by adding the mixture of siRNA and the reagent onto the cells as soon as seeding the cells on the plates (21). Transfection efficiency of this transfection condition was estimated by green fluorescent protein (GFP) signals derived from a sham transfection of pEGFP-N1 Vector (Clontech Laboratories, Palo Alto, CA) to the NB-1 cell. Approximately 30% of the cells were fluorescent. To study the specific effect of *MYCN* silencing, we prepared the following four groups including several types of control: group 1 (*MYCN*-siRNA group), transfected siRNA against human MYCN; group 2 (NC-siRNA group), transfected negative control siRNA; group 3 (mock control group), the cells were treated with the reagent and PBS without any siRNAs to verify the influence of the transfection reagent; group 4 (no treatment group), the cells received no treatment.

RNA and cDNA preparation. The reverse transfection treatment was applied to $2.5x10^5$ NB1 cells suspended in 2 ml medium in each well of a 6-well plate. At a later time indicated below, the cells were harvested for RNA extraction and cDNA synthesis. Total cellular RNA of each group was prepared by RNAqueous RNA isolation kit (Ambion, Austin, TX). First-strand cDNA was synthesized from 1 μg of total RNA using MMLV Reverse Transcriptase (Clontech Laboratories) and oligo(dT) primers.

Gene expression assays by real-time RT-PCR. To quantitate the level of mRNA of the *MYCN* and its relating genes Ha-*ras*, *TrkA*, *TrkB*, and *TrkC* that are associated with differentiation and prognosis of NB, real-time RT-PCR was performed on an ABI PRISM 7700 sequence detection system using Sequence Detector V1.7 software (PE Applied Biosystems Inc., San Jose, CA) (22). Human *GAPDH* was used as an internal control. Primers and TaqMan probes for *MYCN*, Ha-*ras*, *TrkA*, *TrkB*, *TrkC* and *GAPDH* were indicated in Table I. The relative expression levels of *MYCN*, Ha-*ras*, *TrkA*, *TrkB*, and *TrkC* mRNAs were standardized by that of *GAPDH*, and compared to that of no treatment control. *MYCN* mRNA expression was firstly evaluated at post-transfection 48 h, then, time-course of the expression for up to 6 days after transfection was independently investigated. Expressions of the Ha-*ras*, *TrkA*, *TrkB*, and *TrkC* mRNAs were evaluated at 48 h.

Western blotting. Ninety-six hours after siRNA transfection on $1.5x10^5$ NB1 cells under the similar conditions as the gene expression assay, cells of each group were harvested to quantitate the MYCN protein level using Western blotting (23). Briefly, harvested cells were lysed in RIPA lysis buffer (Upstate, Lake Placid, NY) and protein amounts were measured by BCA protein assay set (Pierce Biotechnology, Inc., Rockford, IL). Then, 25 μg of protein was loaded on a 10% sodium dodecyl sulfate-polyacrylamide gel (Criterion™ XT Precast Gel, Bio-Rad, Hercules, CA) for electrophoresis, and subsequently transferred onto a polyvinyl difluoride membrane. The membrane was soaked in a solvent (Can Get Signal, Toyobo, Osaka, Japan) including anti-MYCN monoclonal antibody (Santa Cruz Biotechnology Inc., Santa Cruz, CA) at a dilution of 2.0 μg/ml, and incubated for 24 h at 4°C. The membrane was then incubated with a horseradish

Table I. Primers used in real-time quantitative PCR reactions.

Gene		Sequences (5'→3')
MYCN	Forward	GACCACAAGGCCCTCAGTACC
	Reverse	TGACCACGTCGATTTCTTCCT
	TaqMan probe	FAM-CCGGAGAGGACACCCTGAGCGA-TAMRA
GAPDH[a]	Forward	GAAGGTGAAGGTCGGAGTCA
	Reverse	GAAGATGGTGATGGGATTTC
	TaqMan probe	FAM-CAAGCTTCCCGTTCTCAGCC-TAMRA
TrkA	Forward	TTCACCTACGGCAAGCAGC
	Reverse	CCTGCGTGATGCAGTCGAT
	TaqMan probe	FAM-TGGTACCAGCTCTCCAACACGGAGG-TAMRA
TrkB	Forward	GTCTTTGAGTACATGAAGCATGGG
	Reverse	TCAGCACGGCATCAGGG
	TaqMan probe	FAM-ACCTCAACAAGTTCCTCAGGGCACACG-TAMRA
TrkC	Forward	CAAATATGGTCGACGGTCCAA
	Reverse	GAGTCCTCCTCACCACTGATGAC
	TaqMan probe	FAM-TTTGGAATGAAGGGTCCCGTGGC-TAMRA
Ha-*ras*	Forward	CCAGAACCATTTTGTGGACGA
	Reverse	CCCATCAATGACCACCTGC
	TaqMan probe	FAM-CGACCCCACTATAGAGGATTCCTACCGGA-TAMRA

[a]Human glutaraldehydes-3-phosphate dehydrogenase.

peroxidase conjugated anti-mouse antibody for 1 h and developed with an enhanced chemiluminescence system (Amersham Biosciences Inc., Piscataway, NJ).

Immunocytochemistry. For each group, $3.0x10^4$ NB-1 cells were treated and maintained in 0.5 ml medium per chamber on the four-chamber culture slides (BD Falcon™, BD Biosciences, San Jose, CA). At post-transfection 96 h, the cells were fixed in 4% paraformaldehyde, rinsed in PBS, and permeabilized with 1% Triton X-100 for 1 h. Then, they were incubated with anti-MYCN antibody (2.0 μg/ml) at 4°C overnight after a blockage step of 30 min performed in 10% normal rabbit serum. For visualization, FITC-conjugated rabbit anti-mouse immunoglobulins (6 mg/ml; Dako, Tokyo, Japan) were used as the second antibody, and nuclear staining was done in PBS. The slides were washed and mounted with fluorescence mounting medium (Dako) to be examined with photographs taken by Keyence VB6000 digital photography system (Keyence, Osaka, Japan) attached to Nikon Eclipse C1000 microscope (Nikon, Tokyo, Japan).

Cell viability assay and time-course evaluation. Cell viability was determined by WST-1 assay utilizing a colorimetric detection of mitochondrial dehydrogenase in viable cells (24). NB-1 cells were seeded at a density of $1x10^4$ cells in 100 μl of medium into each well of 96-well plates and maintained without medium change for up to 9 days after transfection. From post-transfection day 1, four wells were devoted for the assay everyday, and time-course of cell viability was monitored. In practice, 10 μl of WST-1 solution (Cell Count Reagent SF, Nacalai tesque) was added to each well, and samples were incubated at 37°C for 2 h. Then, the absorbency of the treated samples against a blank control was measured by an immunoreader apparatus (Immuno Mini NJ-2300, Nippon InterMed, Tokyo, Japan) under 414 nm as a detection wavelength and 630 nm as a reference wavelength, respectively.

Detection of apoptosis. To further assess influence of *MYCN*-siRNA on the cell survival, apoptotic features of NB-1 cells were evaluated. This was performed semi-quantitatively by using the TUNEL principle (ApopTag Plus Fluorescein *In Situ* Apoptosis Detection Kit, Serologicals Corp., Norcross, GA). Cells were similarly seeded and transfected on the culture slides as the immunocytochemistry study. At post-transfection 96 h, the cells on the slides were fixed and subjected to the assay, according to the manufacturer's instructions. Apoptotic cells were observed and counted under a fluorescence microscope. Moreover, we evaluated the percentage of positive apoptosis cells in each group (25).

Morphologic change evaluation. To evaluate morphologic changes of the NB-1 cells induced by siRNA treatments, each group cells were stained with Phalloidin-Tetramethylrhodamine-B-isothiocyanate (Sigma-Aldrich Corp., St. Louis,

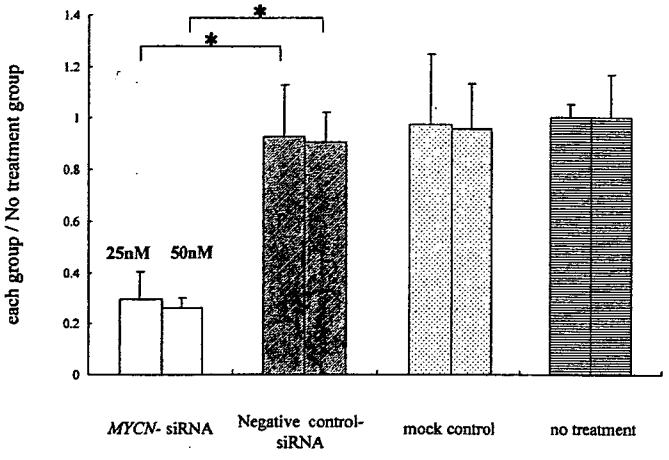

Figure 1. Assessment of relative mRNA expression of *MYCN* by real-time RT-PCR. The expression level of *MYCN* mRNA of the no treatment group defined as 1. The expression level of *MYCN*-siRNA group was significantly reduced to 30% of those of three control groups in NB-1 cell line. No significant change in the NC-siRNA group and mock control group was found compared to the no treatment group. Different *MYCN*-siRNA concentrations (25 and 50 nM) brought similar suppressive effect on the *MYCN* mRNA expression level (*p-value <0.05).

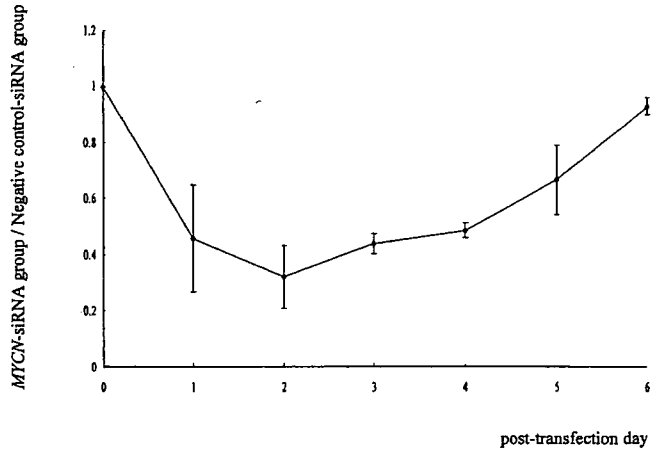

Figure 2. Time-course curve of *MYCN* mRNA expression level after *MYCN*-siRNA treatment. The expression level of the siRNA treated cells relative to that of Negative control-siRNA group on each day was calculated and plotted. Note that the maximum suppression occurred around post-transfection day 2.

MO) at 96 h. This staining highlighted cellular filamentous actin and differentiation appearance of the neuronal cells could be observed under a fluorescence microscope (26).

Statistical analysis. All experiments were performed at least three times and typical results were demonstrated. Data are presented as means together with standard deviation for each parameter. The statistical analysis was performed by an unpaired Student's t-test, and a p-value <0.05 was considered statistically significant.

Results

Effect of siRNA on MYCN mRNA expression. Forty-eight hours after *MYCN*-siRNA transfection, the expression level of *MYCN* mRNA significantly decreased to approximately 30% of group 4 ($p<0.05$) (Fig. 1), whereas the levels observed in groups 2 and 3 were similar to group 4. In these initial experiments, we separately treated the NB-1 cells with different *MYCN*-siRNA concentrations (25 and 50 nM), and found that both concentrations brought similar suppressive effect on the *MYCN* mRNA expression level (Fig. 1). When each of the three *MYCN*-siRNAs (si-*MYCN*-1-3) included in the cocktail was separately used for transfection at 25 nM concentration, we also found that *MYCN* mRNA expression was similarly reduced (data not shown). Then, in our subsequent experiments, we solely used the 25 nM cocktail.

Time-course curve of relative expression of *MYCN* mRNA is shown in Fig. 2. It appeared that *MYCN* knock-down lasted for 6 days after transfection. The nadir level of reduction occurred around post-transfection days 2, and consistently reached 30% of group 2. On post-transfection day 6, the expression of *MYCN* recovered to the same level observed in group 2.

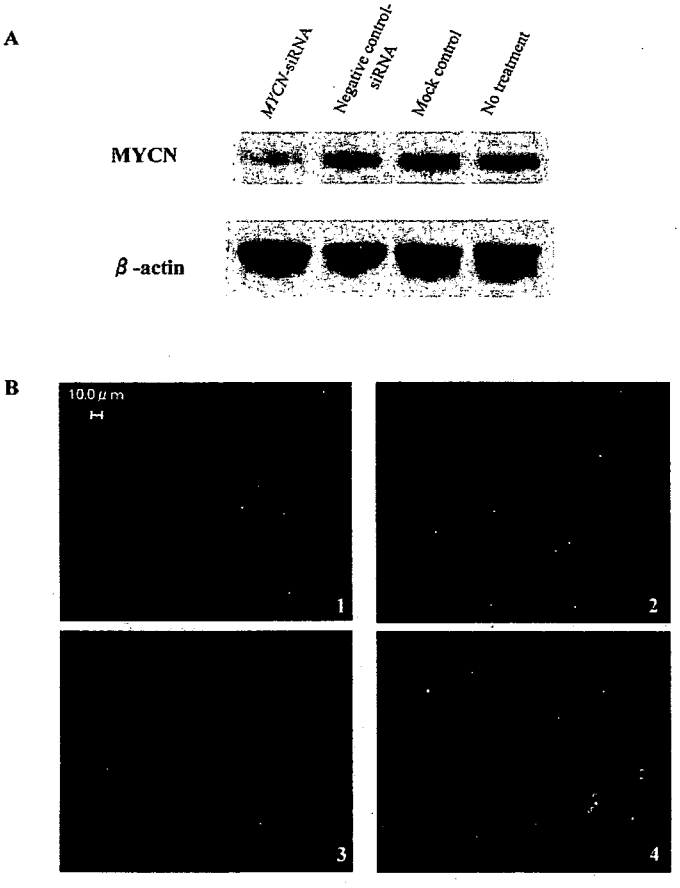

Figure 3. (A), Western blotting of MYCN and ß-actin. The study revealed reduction of cellular MYCN level in NB-1 cells treated by *MYCN*-siRNA. (B), Fluorescent immunocytochemical staining study demonstrating MYCN nuclear staining pattern in NB-1 cells. At 96 h of culture, nuclear staining of MYCN became very faint in the majority of the cells in the *MYCN*-siRNA group, whereas, those in other three control groups, almost all cells showed strong signals. Panel 1, *MYCN*-siRNA group. Panel 2, Negative control-siRNA group. Panel 3, Mock control group. Panel 4, No treatment group.

Western blotting for MYCN. At post-transfection 96 h, Western blot assay revealed a reduction of MYCN protein level in group 1 compared to the other groups. MYCN protein expression did not differ among groups 2, 3 and 4 (Fig. 3A).

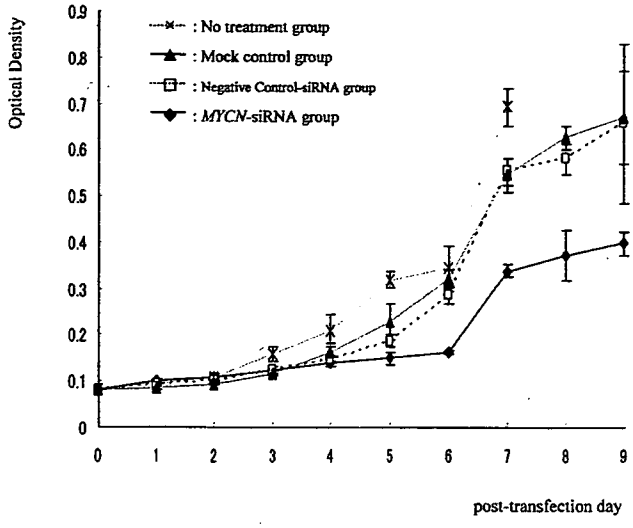

Figure 4. Time-course study assessed by WST-1 method demonstrated a significant reduction of NB-1 cell viability in the *MYCN*-siRNA group from day 5 (p-value <0.05). No significant change was found between the negative control-siRNA group and mock control group.

Immunocytochemistry for MYCN. Immunocytochemistry using anti-MYCN antibody showed intense immunoreactivity of nuclear staining groups 2, 3 and 4. In contrast, 96 h after siRNA treatment, nuclear staining of MYCN became very faint in the majority of the cells in group 1 (Fig. 3B).

RNAi suppressed NB-1 cell proliferation. In WST-1 assay, group 1 showed significantly reduced viable cell numbers, compared to groups 2 and 3. This significant suppression in cell proliferation became apparent on post-transfection day 5 and continued until day 9, when cells reached confluent growth in the NC-siRNA and mock groups and the time-course study was terminated ($p<0.05$) (Fig. 4). Cell proliferation modes of groups 2 and 3 were similar, but less propagated than that observed in group 4, probably reflecting some cytotoxic effect of the transfection reagent.

Apoptosis evaluation. Using *in situ* TUNEL assay, we identified significantly higher proportion of TUNEL positive cells in group 1 compared to the other groups ($p<0.0001$) (Fig. 5A). More than 50 cells per 100 were apoptotic in group 1, compared to 13 cells in group 2, and approximately 5 in groups 3 and 4 (Fig. 5B). These findings may indicate that siRNA treatment against MYCN activates an apoptotic process in NB-1 cells.

Morphological evaluation. Original shape of NB-1 is round. In group 1, the cells treated by *MYCN*-siRNA exhibited multidirectional neurite extension. Additionally, size of these cells and nuclei became apparently larger than those observed in the other cell groups (Fig. 6). These morphologic changes were consistent with neural differentiation.

Relative expression of Ha-ras, TrkA, TrkB and TrkC. At forty-eight hours after the siRNA treatment, relative expressions of *TrkA* and *TrkC* mRNA were significantly up-regulated in group 1 compared with other groups ($p<0.05$). The expression

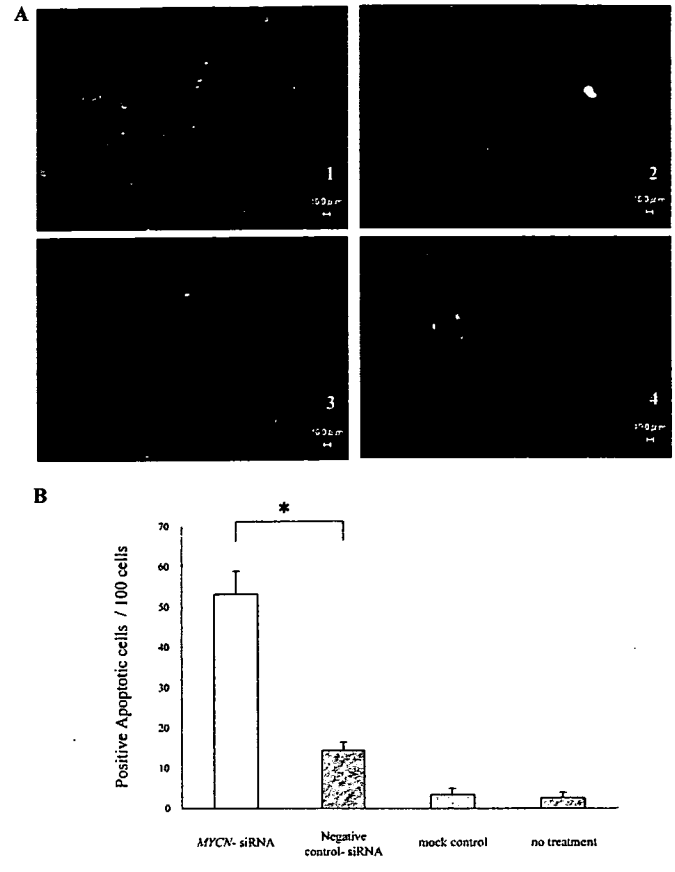

Figure 5. Detection of apoptosis. (A), Effect of *MYCN*-siRNA treatment on NB-1 culture at 96 h. The TUNEL positive cells were observed more frequently in the *MYCN*-siRNA group. Panel 1, *MYCN*-siRNA group. Panel 2, Negative control-siRNA group. Panel 3, Mock control group. Panel 4, No treatment group. (B), Apoptotic cell counting per 100 cells at 96 h. Cells with apoptotic bodies were significantly increased in the *MYCN*-siRNA group (*p-value <0.0001).

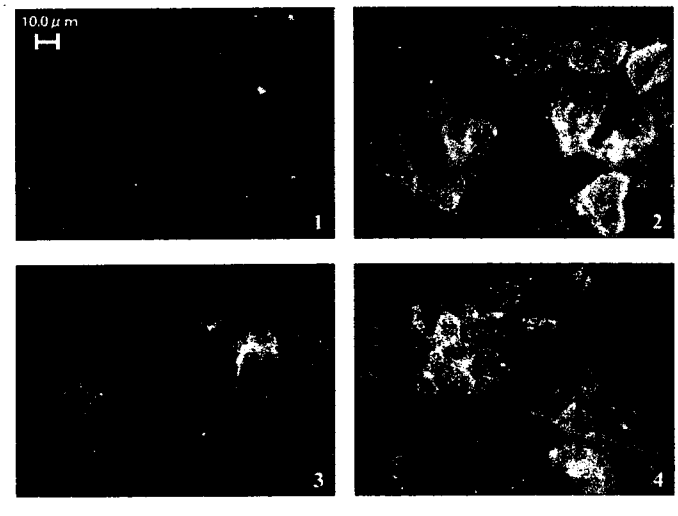

Figure 6. Effect of *MYCN*-siRNA treatment on NB-1 culture at 96 h. Phalloidin-TRTC staining of NB-1 exhibited multidirectional neurite extension in the *MYCN*-siRNA group. Additionally, sizes of the cells and the nucleus in this group became apparently larger than those observed in the other groups. These morphologic changes indicate differentiation effect of *MYCN*-siRNA treatment. Panel 1, *MYCN*-siRNA group. Panel 2, Negative control-siRNA group. Panel 3, Mock control group. Panel 4, No treatment group.

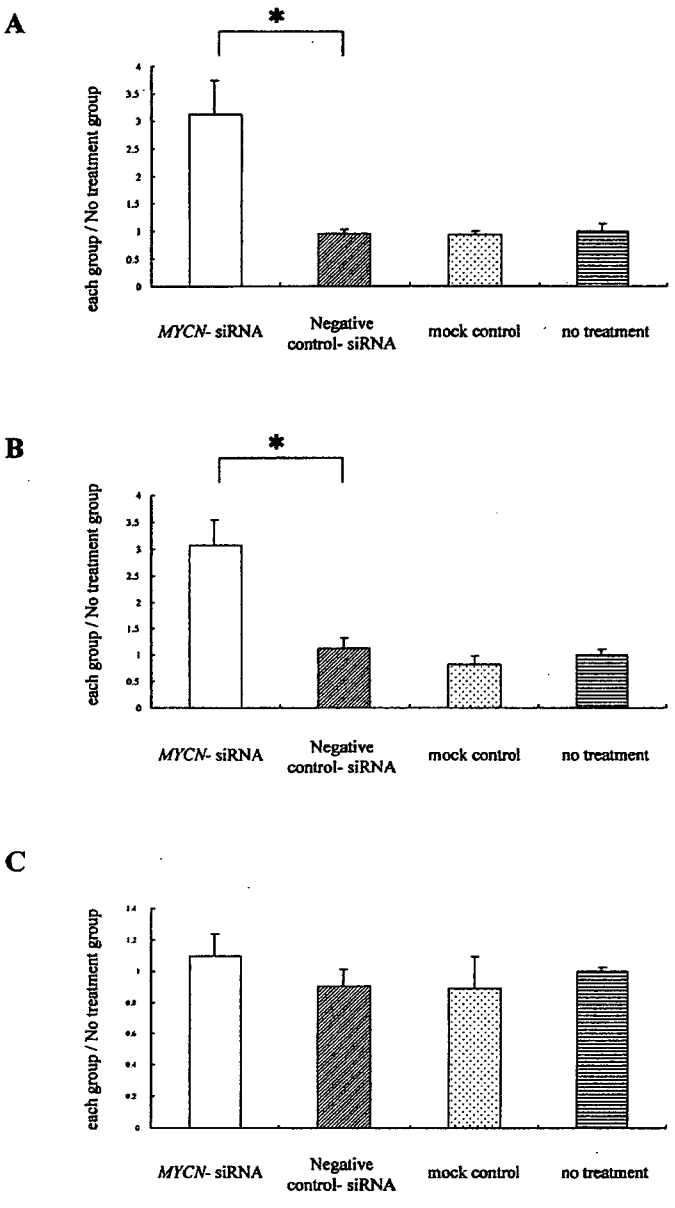

Figure 7. Assessment of relative mRNA expression levels each of *TrkA* (A), *TrkC* (B) and Ha-*ras* (C) by real-time RT-PCR. *TrkA* and *TrkC*, indicators of favorable prognosis, were significantly up-regulated. On the other hand, Ha-*ras* did not show significant change (*p-value <0.05).

of *TrkB* was not detected. The relative expression of Ha-*ras* did not change by the siRNA treatment (Fig. 7).

Discussion

In the present study, by using siRNA treatment, we conducted a knock-down of *MYCN* expression to examine its effect on NB-1 cell line in which the *MYCN* gene is amplified and overexpressed.

siRNA is a synthetic short double-stranded RNA that induces the destruction of homologous single-stranded RNA, when introduced into a cell. Therefore, siRNA has been evaluated as an effective tool for suppressing the target protein by specifically digesting its mRNA (18,27). In our experiment real-time RT-PCR and Western blotting definitely demonstrated that the treatment with siRNA targeted *MYCN* decreased *MYCN* mRNA expression as well as protein expression. Although it was previously reported that knock-down of *MYCN* in NB cells with antisense oligonucleotide against *MYCN* (28-30), siRNA is generally superior to antisense oligonucleotides in terms of efficiency and specificity (31).

Gene transfection into neuronal cells has been generally considered difficult. Biewenga *et al* mentioned that of all mammalian cells, neurons are probably the most difficult to transfect (32). Especially with conventional techniques like calcium-phosphate transfection or lipofection, very poor efficiency is commonly achieved. Biewenga *et al* recommended the biolistic gene transfer technique in which the plasmid DNAs of interest were coated onto small particles, which were accelerated by a particular driving force. However, they were able to achieve only up to 2% of transfection efficacy for gene transfer into NB cell lines (32).

To solve this problem, we adopted a reverse transfection method, in which cell seeding and transfection were performed simultaneously by adding the mixture of siRNA and the reagent onto the cells as soon as the cells had been seeded on the plates (21). Although we employed modified reagent for lipofection, reverse transfection method successfully achieved transfection efficacy around 30% and resulted in 70% reduction of *MYCN* expression. Our results show that reduction of *MYCN* mRNA expression induce growth inhibition of NB-1 cells.

After reduction of MYCN protein expression, the expression of target genes of *MYCN*, such as *ODC, MCM7* and *MRP1*, was probably suppressed. Those genes usually lead to cell progression through the G1 phase of the cell cycle (17,33,34). Thus, reduction of those gene expressions may lead to G1 cell cycle arrest and results in the suppression of cell proliferation.

To investigate whether an apoptotic pathway was involved in suppression of cell proliferation after silencing of *MYCN*, we conducted TUNEL assay and confirmed that significantly higher proportion of TUNEL positive cells were observed in siRNA treated NB-1 cells. Galderisi *et al* showed that antisense oligonucleotide treatment of substrate adherent NB cells (S cells) resulted in a clear increase of the proapoptic Bax and Bak gene expression, along with a drastic decrease in the level of anti-apoptic Bcl-2 mRNA (35). Thus, these genes may have important roles in cell death after *MYCN* gene inhibition. Galderisi *et al* also found that the differentiation and apoptosis that followed antisense treatment persisted after the end of *MYCN* gene inhibition, indicating that a lasting *MYCN* downregulation is not required to induce these processes (35).

Moreover, after transfection with *MYCN*-siRNA we also observed that a pattern of the outgrowth was mostly multidirectional neurite extension of cell processes, and gradual long neurite elongation. Additionally, sizes of the cells and the nucleus in this group became larger than those observed in the other groups. These morphologic changes indicate differentiation effect of *MYCN*-siRNA treatment. Similarly previous studies had reported that *MYCN* suppression using antisense oligonucleotides resulted in cell differentiation in NB (28,30,35,36). These studies suggested that alterations in the regulation of *MYCN* expression can modulate the differentiation process of NB cells (28).

After silencing of *MYCN* expression by RNA interfering, relative expressions of *TrkA* and *TrkC* mRNA were significantly up-regulated. At the same time, morphological change corresponded to tendency of differentiation was observed. Evidence from several independent studies suggests that high expression of *TrkA* is an indicator of favorable outcome, and there is an inverse correlation between *TrkA* expression and *MYCN* amplification. *TrkC* is expressed in favorable NBs, essentially all of which also express *TrkA* (37-39). These findings suggest that suppression of *MYCN* up-regulated *TrkA* which activate specific signaling pathways linking to differentiation and survival.

Ha-*ras* genes are also closely associated with the growth, differentiation, and survival of neuronal tissues. Several observations suggest a role of Ha-*ras* p21 in promoting cellular differentiation and suppression of the proliferation activity of PC12, a tumor cell line originating from rat sympathetic nerve tissue (40). Thus, we examined Ha-*ras* expression after *MYCN* silencing. Consequently, expression of Ha-*ras* mRNA did not increase. Therefore, the differentiation after silencing *MYCN* may have a relation not to Ha-*ras* but rather to *TrkA* cascade.

In conclusion, the expression level of the *MYCN* mRNA was significantly reduced using the RNAi method. As a result, the knock-down of *MYCN* expression induced growth-inhibition, apoptotic activity and cell differentiation in *MYCN*-amplified NB-1 cell line. These data indicate that *MYCN* might be the key factor in the tumorigenesis and prognosis of NBs. Thus, silencing the *MYCN* gene by the RNAi method could be a potential tool for the treatment of NBs with *MYCN* amplification in the future.

Acknowledgements

This study was partially supported by a Grant-in-Aid from the Ministry of Education, Science, Sports and Culture of Japan (grant no. 17591861).

References

1. Gurney JG, Ross JA, Wall DA, Bleyer WA, Severson RK and Robison LL: Infant cancer in the U.S.: histology-specific incidence and trends, 1973 to 1992. J Pediatr Hematol Oncol 19: 428-432, 1997.
2. Matthay KK: Neuroblastoma: a clinical challenge and biologic puzzle. CA: Cancer J Clin 45: 179-192, 1995.
3. Young JL Jr and Miller RW: Incidence of malignant tumors in U.S. children. J Pediatr 86: 254-258, 1975.
4. Kawa K, Ohnuma N, Kaneko M, *et al*: Long-term survivors of advanced neuroblastoma with MYCN amplification: a report of 19 patients surviving disease-free for more than 66 months. J Clin Oncol 17: 3216-3220, 1999.
5. Matthay KK, Villablanca JG, Seeger RC, *et al*: Treatment of high-risk neuroblastoma with intensive chemotherapy, radiotherapy, autologous bone marrow transplantation, and 13-cis-retinoic acid. Children's Cancer Group. N Engl J Med 341: 1165-1173, 1999.
6. Lu X, Pearson A and Lunec J: The MYCN oncoprotein as a drug development target. Cancer Lett 197: 125-130, 2003.
7. Westermann F and Schwab M: Genetic parameters of neuroblastomas. Cancer Lett 184: 127-147, 2002.
8. Schwab M, Varmus HE, Bishop JM, *et al*: Chromosome localization in normal human cells and neuroblastomas of a gene related to c-myc. Nature 308: 288-291, 1984.
9. Brodeur GM, Seeger RC, Schwab M, Varmus HE and Bishop JM: Amplification of N-myc in untreated human neuroblastomas correlates with advanced disease stage. Science 224: 1121-1124, 1984.
10. Nakagawara A and Ikeda K: N-myc oncogene amplification and catecholamine metabolism in children with neuroblastoma. Lancet i: 559, 1987.
11. Nisen PD, Waber PG, Rich MA, *et al*: N-myc oncogene RNA expression in neuroblastoma. J Natl Cancer Inst 80: 1633-1637, 1988.
12. Bordow SB, Norris MD, Haber PS, Marshall GM and Haber M: Prognostic significance of MYCN oncogene expression in childhood neuroblastoma. J Clin Oncol 16: 3286-3294, 1998.
13. Slavc I, Ellenbogen R, Jung WH, *et al*: myc gene amplification and expression in primary human neuroblastoma. Cancer Res 50: 1459-1463, 1990.
14. Cohn SL, London WB, Huang D, *et al*: MYCN expression is not prognostic of adverse outcome in advanced-stage neuroblastoma with nonamplified MYCN. J Clin Oncol 18: 3604-3613, 2000.
15. Matthay KK: MYCN expression in neuroblastoma: a mixed message? J Clin Oncol 18: 3591-3594, 2000.
16. Weiss WA, Aldape K, Mohapatra G, Feuerstein BG and Bishop JM: Targeted expression of MYCN causes neuroblastoma in transgenic mice. EMBO J 16: 2985-2995, 1997.
17. Manohar CF, Bray JA, Salwen HR, *et al*: MYCN-mediated regulation of the MRP1 promoter in human neuroblastoma. Oncogene 23: 753-762, 2004.
18. Fire A, Xu S, Montgomery MK, Kostas SA, Driver SE and Mello CC: Potent and specific genetic interference by double-stranded RNA in *Caenorhabditis elegans*. Nature 391: 806-811, 1998.
19. Scherr M, Morgan MA and Eder M: Gene silencing mediated by small interfering RNAs in mammalian cells. Curr Med Chem 10: 245-256, 2003.
20. Dorsett Y and Tuschl T: siRNAs: applications in functional genomics and potential as therapeutics. Nat Rev Drug Discov 3: 318-329, 2004.
21. Ovcharenko D, Jarvis R, Hunicke-Smith S, Kelnar K and Brown D: High-throughput RNAi screening *in vitro*: from cell lines to primary cells. RNA 11: 985-993, 2005.
22. Tanaka S, Tajiri T, Noguchi S, *et al*: Clinical significance of a highly sensitive analysis for gene dosage and the expression level of MYCN in neuroblastoma. J Pediatr Surg 39: 63-68, 2004.
23. Ohno S, Nishi T, Kojima Y, Haraoka J, Ito H and Mizuguchi J: Combined stimulation with interferon alpha and retinoic acid synergistically inhibits proliferation of the glioblastoma cell line GB12. Neurol Res 24: 697-704, 2002.
24. Ishiyama M, Tominaga H, Shiga M, Sasamoto K, Ohkura Y and Ueno K: A combined assay of cell viability and *in vitro* cytotoxicity with a highly water-soluble tetrazolium salt, neutral red and crystal violet. Biol Pharm Bull 19: 1518-1520, 1996.
25. Tonelli R, Purgato S, Camerin C, *et al*: Anti-gene peptide nucleic acid specifically inhibits MYCN expression in human neuroblastoma cells leading to cell growth inhibition and apoptosis. Mol Cancer Ther 4: 779-786, 2005.
26. Fan S, Ramirez SH, Garcia TM and Dewhurst S: Dishevelled promotes neurite outgrowth in neuronal differentiating neuroblastoma 2A cells, via a DIX-domain dependent pathway. Brain Res 132: 38-50, 2004.
27. Tijsterman M and Plasterk RH: Dicers at RISC; the mechanism of RNAi. Cell 117: 1-3, 2004.
28. Negroni A, Scarpa S, Romeo A, Ferrari S, Modesti A and Raschella G: Decrease of proliferation rate and induction of differentiation by a MYCN antisense DNA oligomer in a human neuroblastoma cell line. Cell Growth Differ 2: 511-518, 1991.
29. Kuss BJ, Corbo M, Lau WM, Fennell DA, Dean NM and Cotter FE: *In vitro* and *in vivo* downregulation of MRP1 by antisense oligonucleotides: a potential role in neuroblastoma therapy. Int J Cancer 98: 128-133, 2002.
30. Schmidt ML, Lal A and Dittmann D: Differential expression in an antisense MYCN neuroblastoma model. Med Pediatr Oncol 35: 669-672, 2000.
31. Miyagishi M, Hayashi M and Taira K: Comparison of the suppressive effects of antisense oligonucleotides and siRNAs directed against the same targets in mammalian cells. Antisense Nucleic Acid Drug Dev 13: 1-7, 2003.
32. Biewenga JE, Destree OH and Schrama LH: Plasmid-mediated gene transfer in neurons using the biolistics technique. J Neurosci Methods 71: 67-75, 1997.
33. Brodeur GM: Neuroblastoma: biological insights into a clinical enigma. Nat Rev 3: 203-216, 2003.

34. Peaston AE, Gardaneh M, Franco AV, *et al*: MRP1 gene expression level regulates the death and differentiation response of neuroblastoma cells. Br J Cancer 85: 1564-1571, 2001.
35. Galderisi U, Di Bernardo G, Melone MA, *et al*: Antisense inhibitory effect: a comparison between 3'-partial and full phosphorothioate antisense oligonucleotides. J Cell Biochem 74: 31-37, 1999.
36. Schmidt ML, Salwen HR, Manohar CF, Ikegaki N and Cohn SL: The biological effects of antisense N-myc expression in human neuroblastoma. Cell Growth Differ 5: 171-178, 1994.
37. Nakagawara A, Arima M, Azar CG, Scavarda NJ and Brodeur GM: Inverse relationship between trk expression and N-myc amplification in human neuroblastomas. Cancer Res 52: 1364-1368, 1992.
38. Nakagawara A, Arima-Nakagawara M, Scavarda NJ, Azar CG, Cantor AB and Brodeur GM: Association between high levels of expression of the TRK gene and favorable outcome in human neuroblastoma. N Engl J Med 328: 847-854, 1993.
39. Brodeur GM, Nakagawara A, Yamashiro DJ, *et al*: Expression of TrkA, TrkB and TrkC in human neuroblastomas. J Neurooncol 31: 49-55, 1997.
40. Tanaka T, Sugimoto T and Sawada T: Prognostic discrimination among neuroblastomas according to Ha-ras/trk A gene expression: a comparison of the profiles of neuroblastomas detected clinically and those detected through mass screening. Cancer 83: 1626-1633, 1998.

Pediatr Surg Int (2007) 23:1203–1207
DOI 10.1007/s00383-007-2065-9

ORIGINAL ARTICLE

Intraoperative radiation therapy for advanced neuroblastoma: the problem of securing the IORT field

Kiminobu Sugito · Takeshi Kusafuka · Mayumi Hoshino · Mikiya Inoue · Hiroshi Goto · Taro Ikeda · Noritsugu Hagiwara · Tsugumichi Koshinaga · Masahiro Fukuzawa · Masanori Nakamura · Hiroyuki Shichino · Motoaki Chin · Hideo Mugishima · Tsutomu Saito · Yoshiaki Tanaka

Accepted: 28 September 2007 / Published online: 30 October 2007

Abstract To evaluate the efficacy of intraoperative radiation therapy (IORT) and the problem of securing the IORT field in advanced pediatric neuroblastoma. Between 1996 and 2005, 12 children received IORT for advanced pediatric neuroblastoma patients. Electron beam energies ranged from 10 to 12 MeV and median dose was 10 Gy (8–12 Gy). All of them had surgery with IORT against the primary tumor site and the abdominal aorta surroundings. A gross total resection (GTR) was achieved in 10 patients and subtotal resection (STR) was two patients. All of 12 patients were classified as high risk. Nine patients were alive 17–120 (mean 48 months) after diagnosis. Local tumor control was achieved in 100% of patients, of whom one experienced local recurrence outside the IORT field. At the operation, it was difficult to secure the IORT field because of the angle of the radiation cylinder in three patients. One of the three of these patients experienced local recurrence outside of the IORT field in the upper side of superior mesenteric artery and two of three patients had an external beam radiation after surgery, and there was no local recurrence. One patient had a postoperative ileus, and one patient had transient diarrhea and hydronephrosis. For advanced neuroblastoma patients, IORT produced excellent local control after surgery. However, there is a problem of securing the IORT field. For local control, it is necessary to add an external beam radiation after IORT when it is difficult to secure the IORT field.

Keywords Intraoperative radiation therapy · Neuroblastoma · External beam radiation therapy

K. Sugito (✉) · T. Kusafuka · M. Hoshino · M. Inoue · H. Goto · T. Ikeda · N. Hagiwara · T. Koshinaga · M. Fukuzawa
Department of Pediatric Surgery, Nihon University School of Medicine, 30-1, Ohyaguchi-Kamimachi, Itabashi-ku, Tokyo 173-8610, Japan
e-mail: ksugito@hotmail.com

M. Nakamura · H. Shichino · M. Chin · H. Mugishima
Department of Pediatrics, Nihon University School of Medicine, Tokyo, Japan

T. Saito · Y. Tanaka
Department of Radiology, Nihon University School of Medicine, Tokyo, Japan

Introduction

In intraoperative radiation therapy (IORT) a high single radiation dose is delivered to the tumor site with protection of normal uninvolved organs and tissues [1–6]. Neuroblastoma is the most common solid tumor in childhood [7]. The clinical significance of intensive surgical therapy as a means to control the local lesion has been controversial in the treatment of advanced neuroblastoma [8, 9]. Renal vascular problems and other major complications were reported after extensive surgical resection of neuroblastoma [10, 11]. To prevent the major complications of the surgical treatment and excessive lymphadenectomy, we have been doing IORT. To evaluate the efficacy and problem of IORT in advanced pediatric neuroblastoma, our 10-year experience of IORT was reviewed in this study.

Materials and methods

Between 1996 and 2005, 12 patients received IORT for pediatric advanced neuroblastoma. The international neuroblastoma staging system (INSS) [12, 13] was determined for this study by retrospective interpretation of clinical,

Table 1 Induction chemotherapy regimens for advanced neuroblastoma following to JANB (≥1 year old) (mg/m^2)

MYCN status	1996–1997		1998–2005
	N-*myc*		All patients
	<10 copies	≥10 copies	
Regimen	91A1	91A3	98A3
Cyclophoshamide	1,200 × 1	1,200 × 2	1,200 × 2
Vincristine			1.5 × 1
Etoposide	100 × 5	100 × 5	
Pirarubicine	40 × 1	40 × 1	40 × 1
Cisplatin	90 × 1	25 × 5	25 × 5

radiological and surgical data. Shimada classification [14] was recorded by chart review and by blinded histopathological review of pathology specimens. N-*myc* copy number was recorded by chart review. At first we performed open biopsy for classification and diagnosis in all cases. After the diagnosis, all patients received induction chemotherapy with combination of cyclophoshamide, vincristine, etoposide, pirarubicine, and cisplatin, and according to the protocol proposed by the Japanese study group for advanced neuroblastoma (JANB) [15] (Table 1). After six courses of induction chemotherapy, a radical operation with IORT was performed. Response to induction chemotherapy was determined by magnetic resonance imaging (MRI) or computed tomographic (CT) scan, ^{131}I-meta-iodobenzylguanidine (MIBG) scan, bone scan and bilateral bone-marrow biopsies. Ten of 12 patients had peripheral blood stem cell transplantation (PBSCT) and seven of 12 patients had total body irradiation (TBI) preoperatively.

The second operation was planed in the special IORT operating room. IORT was delivered in a linear accelerator chamber using high-energy electrons between 10 and 12 MeV. The radiation dose delivered was between 8 and 12 Gy. Depending on the depth of treatment desired, the energy levels used were modulated to attain a tissue penetration of 1–3 cm below the surface of the IORT field. At this point two surgeons and radiotherapist placed a radiation tube for localized irradiation under sterile conditions above the primary tumor site and the abdominal aorta surroundings leaving all other organs out of the IORT field, and the IORT team exited the room during the 2- to 3-min IORT delivery time while the patients and monitors were continuously observed via closed-circuit television. Special attention was given to the duodenum, small intestine, kidney, ureter and pancreas, which are susceptible to radiation. When we judged IORT to be insufficient for the primary tumor site during radical operation, we added external beam radiation therapy (EBRT) of 20 Gy within 1 month after IORT.

The clinical feathers and outcomes were analyzed retrospectively in relation to the control of the IORT field.

Results

Patient summary (Table 2)

Between 1996 and 2005, we treated 12 patients with neuroblastoma (nine with stage 4, three with stage 3 (INSS), who had tumor resection with IORT (8–12 Gy, 10–12 MeV of electron beam) against the primary tumor site and the abdominal aorta surroundings in our hospital. The age of patients at initial diagnosis ranged from 1 to 10 years (median 5.2 years), and included six boys and six girls. The primary tumors were located in the adrenal grand in nine cases and retroperitoneum in three cases. A complete gross surgical resection was achieved in 10 of 12 patients who received IORT during a second surgical procedure. While 10 patients had complete gross tumor resection at the time of the second operation, five of these patients did not have viable tumor on histopathologic examination (patients7, 8, 9, 10, and 11).

Pathological criteria relating to Shimada classification and N-*myc* copy number was available in all of 12 patients. All three patients with stage 3 had unfavorable criteria. One of these three patients with stage 3 showed N-*myc* oncogene amplification. Six of nine patients with stage 4 had unfavorable criteria. Two of nine patients with stage 4 showed N-*myc* oncogene amplification (also with unfavorable Shimada classification). Seven patients of all 12 patients had MIBG hot lesion before IORT (Patients 1, 2, 4, 5, 6, and 12). There were three patients who did not normalize the tumor marker (such as [Vanillylmandelic acid (VMA), homovanillic acid (HVA)]), and NSE (neuron-specific enolase) after induction chemotherapy (Patients 1, 6, and 12). All of these three patients who did not normalize the tumor marker died of relapse (patients 1, 6, and 12).

There was no recurrence of disease in the IORT field in all of 12 patients with median follow-up of 44.2 months (range 17–120). At the time of IORT, seven of these 12 patients had viable tumor seen (patients 1, 2, 3, 4, 5, 6, and 12). There were three children who died of relapse in this study, and these three patients were included in the seven patients who had viable tumor at the time of IORT. There was one patient who had died of local recurrence (patient 12). She had local recurrence outside of the IORT field in the upper side of superior mesenteric artery after IORT and complicated the liver metastasis. The complication rate by IORT in this study was exceedingly low. One patient had postoperative ileus, which required treatment with ileus tube, and one patient had colitis and hydronephrosis.

Table 2 Patients summary

Patient	Sex	Age (year)	Primary site	Stage (INSS)	Extent of resection	Viable tumor in resected specimen Y or N	Shimada classification F or UF	N-*myc* oncogene copy no.	MIBG hot legion before IORT	NSE level before IORT	External Beam radiation	Complication	Survival status months A or D	FU months
1	Female	10	Adrenal	4	STR	Y	UF	1	Primary lesion	29	–	–	D	37
2	Male	9	Adrenal	4	GTR	Y	UF	1	Primary lesion	10	–	–	A	120
3	Female	9	Adrenal	3	GTR	Y	UF	1	Negative	3.7	–	–	A	65
4	Male	3	Retroperitoneum	4	GTR	Y	UF	1	Primary lesion, bone	10	–	Colitis, hydronephrosis	A	54
5	Female	7	Adrenal	4	GTR	Y	UF	1	Primary lesion	9	–	–	A	56
6	Female	3	Adrenal	4	GTR	Y	F	2–9	Primary lesion, bone	20	–	–	D	36
7	Male	5	Adrenal	4	GTR	N	F	1	Negative	10	–	Ileus	A	36
8	Female	1	Adrenal	4	GTR	N	UF	100	Negative	7.7	–	–	A	30
9	Male	2	Adrenal	4	GTR	N	UF	2–9	Negative	10	+	–	A	24
10	Male	3	Retroperitoneum	4	GTR	N	UF	150	Negative	10	+	–	A	17
11	Male	6	Retroperitoneum	3	STR	N	UF	2–9	Negative	7.6	–	–	A	33
12	Female	4	Adrenal	3	GTR	Y	UF	150	Primary lesion	15	–	–	D	22

INSS the international neuroblastoma staging system, *STR* subtotal resection, *GTR* gross total resection, *Y* yes, *N* no, *F* favorable, *UF* unfavorable, *NSE* level of neuron-specific enolase, *A* alive, *D* dead, *FU* follow-up

Although many patients received IORT to paraspinous field, no neuropathies have been seen.

The problem to secure the IORT field

At the time of the IORT, it was difficult to secure the radiation field because of the angle of the radiation cylinder in three patients (patients 9, 10, and 12). Patient 12 had a local recurrence outside of the IORT field in the upper side of superior mesenteric artery after IORT, and so we added the EBRT after the IORT to patient 9 and 10 because it was difficult to secure the IORT field. Neither of these two patients who had the EBRT after the IORT had any local recurrence.

Discussion

Intraoperative radiation therapy has been demonstrated to have an impact on local tumor control in a variety of adult cancers [16–18]. Recently IORT has been described in a cohort of pediatric patients with varying benign conditions and malignancy [5]. EBRT also has been described that it was effective in advanced neuroblastoma [19–21]. The importance of intensive local treatment for advanced neuroblastoma was emphasized in other studies [22–26]. In this study we have been able to evaluate the impact of IORT in 12 children diagnosed with advanced neuroblastoma over a 10-year period. Neuroblastoma already has several well-recognized prognostic factors such as age at diagnosis [26], amplification of the N-*myc* oncogene [27], and Shimada classification of diagnostic tissue [14, 28]. Open biopsy was used for diagnosis in all patients, and we could have data in all patients. The outcome for the patients reported in this study does relate to the histopathological characteristic at diagnosis with eight children with unfavorable Shimada classification surviving. One of the three patients who died had favorable Shimada classification. All of the three patients who had been admitted amplification of the N-*myc* oncogene had unfavorable Shimada classification, and one of them died of the local recurrence (patient 12). The prognosis of the patient who had been admitted unfavorable Shimada classification and amplification of the N-*myc* oncogene was in the bad run though it was not possible to say indiscriminately because the number of cases was little. All of the three patients who died had variable tumors at the point of IORT, though intensive chemotherapy was done. At the point of IORT, it seemed that the existence of variable tumor influenced the prognosis. Non-normalization of the tumor marker after induction chemotherapy and the existence of variable tumors at the point of IORT suggest that there is a possibility that the tumor cell exists locally and systemically and the prognosis is bad. Thinking about patient 12 who had local recurrence outside of IORT field in the upper side of superior mesenteric artery, seemed that we should add EBRT to para-aorta because it was difficult to secure the IORT field. When it was difficult to secure the IORT field and the variable tumor exists in addition to amplification of the N-*myc* oncogene, it seemed that it was necessary to add EBRT to para-aorta or supplemental chemotherapy to control the local part after IORT and it is important to improve the clinical outcome in advanced neuroblastoma. The combination IORT and EBRT appeared effective in advanced neuroblastoma for local control. Some investigators have attributed some complications of IORT and EBRT. These include episodes of intestinal bleeding, neuropathy, increased infection, and secondary neoplasms [29–33]. We did not show any of these complications in our series. We have virtually always been able to dissect the ureter off the tumor and exclude it from the IORT field. But one patient (patient 4) had hydronephrosis on both sides after the IORT.

Intraoperative radiation therapy seems to promote the local control in advanced neuroblastoma. The observation time, however, is still short and our series of patients rather small. Therefore, it is necessary to continue this study to evaluate the role of IORT in advanced neuroblastoma.

References

1. Calvo FA, Sierrasesumaga L, Martin I et al (1989) Intraoperative radiotherapy in the multidisciplinary treatment of pediatric tumors. A preliminary report on initial results. Acta Oncol 28:257–260
2. Abe M, Takahashi M, Yabumoto E et al (1980) Clinical experiences with intraoperative radiotherapy of locally advanced cancers. Cancer 45:40–48
3. Rosen EM, Cassady JR, Frantz CN et al (1984) Neuroblastoma: the joint center for radiation therapy/Dana-Farber Cancer Institute/Children's hospital experience. J Clin Oncol 2:719–732
4. Calvo FA, Ortiz de Urbina D, Sierrasesumaga L et al (1991) Intraoperative radiotherapy in the multidisciplinary treatment of bone sarcomas in children and adolescents. Med Pediatr Oncol 19:478–485
5. Haase GM, Meagher DP Jr, McNeely LK et al (1994) Electron beam intraoperative radiation therapy for pediatric neoplasm. Cancer 74:740–747
6. aufman BH, Gunderson LL, Evans RG et al (1984) Intraoperative irradiation: a new technique in pediatric oncology. J Pediatr Surg 19:861–862
7. Brodeur GM, Gastleberry RP (1993) Neuroblastoma. In: Pizzo PA, Poplack DG (eds) Principles and practice of pediatric oncology. J. B. Lippincott Company, Philadelphia, pp 739–767
8. Kuroda T, Saeki M, Honna T et al (2003) Clinocal significance of intensive surgery with intraoperative radiation for advanced neuroblastoma: does it really make sense?. J Pediatr Surg 38:1735–1738
9. Mugishima H, Iwata M, Okabe I et al (1995) Intra-operative radiation therapy in autotransplant for neoroblastoma. Acta Paediatr Jpn 37:122–124

10. Day DL, Johnson RT, Odrezin GT et al (1991) Renal atrophy or infarction in children with neuroblastoma. Radiology 180:493–495
11. Canete A, Jovani C, Lopez A et al (1998) Surgical treatment for neuroblastoma: complications during 15 years experience. J Pediatr Surg 33:1526–1530
12. Brodeur GM, Seeger RC, Barrett A et al (1988) International criteria for diagnosis, staging and response to treatment in patients with neuroblastoma. Prog Clin Biol Res 271:509–524
13. Brodeur GM, Pritchard J, Berthold F et al (1993) Revisions of the international criteria for neuroblastoma diagnosis, staging, and response to treatment. J Clin Oncol 11:1466–1477
14. Evans AE, D'Angio GJ, Propert K et al (1987) Prognostic factor in neuroblastoma. Cancer 59:1853–1859
15. Sawaguchi S, Kaneko M, Uchino J et al (1990) Treatment of advanced neuroblastoma with emphasis on intensive induction chemotherapy. a report from the study group of Japan. Cancer 66:1879–1887
16. Hoekstra HJ, Sindelar WF, Kinsella TJ (1988) Surgery with intraoperative radiotherapy for sarcomas of the pelvic girdle: a pilot experience. Int J Radiat Oncol Biol Phys 15:1013–1016
17. Gilly FN, Romestaing PJ, Gerard JP et al (1990) Experience of three years with intra-operative radiation therapy using the Lyon intra-operative device. Int Surg 75:84–88
18. Freeman SB, Hamaker RC, Singer MI et al (1990) Intraoperative radiotherapy of head and neck cancer. Arch Otolaryngol Head Neck Surg 116:165–168
19. Schmidt M, Simon T, Hero B et al (2006) Is there a benefit of 131 I-MIBG therapy in the treatment of children with stage 4 neuroblastoma? A retrospective evaluation of the German neuroblastoma trial NB97 and implications for the German neuroblastoma trial NB2004. Nuklearmedizin 24:145–151
20. Siomn T, Hero B, Bongartz R et al (2006) Intensified external-beam radiation therapy improves the outcome of stage 4 neuroblastoma in children >1 year with residual local disease. Strahlenther Onkol 182:389–394
21. von Allmen D, Grupp S, Diller L et al (2005) Aggressive surgical therapy and radiotherapy for patients with high-risk neuroblastoma treated with rapid sequence tandem transplant. J Pediatr Surg 40:936–941
22. Matthay KK, Atkinson JB, Stram DO et al (1993) Patterns of relapse after autologous purged bone marrow transplantation for neuroblastoma: a childrens cancer group pilot study. J Clin Oncol 11:2226–2233
23. La Quaglia MP, Kushner BH, Heller G et al (1994) Stage 4 neuroblastoma diagnosed at more than 1 year of age: gross total resection and clinical outcome. J Pediatr Surg 29:1162–1165
24. Castel V, Tovar JA, Costa E et al (2002) The role of surgery in stage IV neuroblastoma. J Pediatr Surg 37:1574–1578
25. Kuroda T, Saeki M, Honna T et al (2003) Clinical significance of intensive surgery with intraoperative radiation for advanced neuroblastoma: does it really make sense? J Pediatr Surg 38:1735–1738
26. Hassenbusch S, Kaizer H, White JJ (1976) Prognostic factors in neuroblastic tumors. J Pediatr Surg 11:287–297
27. Look AT, Hayes FA, Shuster JJ et al (1991) Clinical relevance of tumor cell ploidy and N-myc gene amplification in childhood neuroblastoma: a pediatric oncology group study. J Clin Oncol 9:581–591
28. Shimada H, Chatten J, Newton WA Jr et al (1984) Histopathologic prognostic factors in neuroblastic tumors: definition of subtypes of ganglioneuroblastoma and an age-linked classification of neuroblastomas. J Natl Cancer Inst 73:405–416
29. Sindelar WF, Kinsella TJ, Hoekstra H et al (1985) Duodenal hemorrhage as a complication of intraoperative radiotherapy for unresectable carcinoma of the pancreas. Proc Am Soc Clin Oncol 4:277
30. Shipley WU, Wood WC, Tepper JE et al (1984) Intraoperative electron beam irradiation for patients with unresectable pancreatic carcinoma. Ann Surg 200:289–296
31. Willett CG, Suit HD, Tepper JE et al (1991) Intraoperative electron beam radiation therapy for retroperitoneal soft tissue sarcoma. Cancer 68:278–283
32. Paulino AC, Ferenci MS, Chiang KY et al (2006) Comparison of conventional to intensity modulated radiation therapy for abdominal neuroblastoma. Pediatr Blood Cancer 46:739–744
33. Paulino AC, Fowler BZ (2005) Secondary neoplasms after radiotherapy for a childhood solid tumor. Pediatr Hematol Oncol 22:89–101

Outcome of Early Surgery for Bilateral Congenital Cataracts in Eyes with Microcornea

SACHIKO NISHINA, EIICHIRO NODA, AND NORIYUKI AZUMA

• PURPOSE: To report the outcome of early surgery for bilateral congenital cataracts in eyes with microcornea.
• DESIGN: Interventional case series.
• METHODS: We retrospectively reviewed 22 eyes of 11 patients with microcorneas who underwent early surgery for bilateral congenital cataracts. All patients underwent lensectomy and anterior vitrectomy via the limbal approach by 12 weeks of age. The corneal diameters at the time of surgery ranged from 7.0 to 9.0 mm. The mean age at the time of surgery was 7.7 ± 3.3 weeks (range, two to 12 weeks); the follow-up period was 115 ± 58 months (range, 40 to 199 months). Aphakic eyes were corrected with spectacles or contact lenses. Visual acuities and the postoperative complications were evaluated periodically.
• RESULTS: The morphologic types of cataract were nuclear (12 eyes), complete (eight eyes), and membranous (two eyes). Other preoperative ocular abnormalities included iris hypoplasia in 10 eyes and persistent fetal vasculature in three eyes. Systemic abnormalities were found in four patients. Postoperative complications occurred in 11 eyes (50%), including glaucoma (nine eyes), exudative retinal detachment (two eyes), rhegmatogenous retinal detachment, and secondary membrane formation, in one eye each. The binocular visual acuity was 20/40 to 20/20 in six patients (55%), 20/200 to 20/100 in two patients (18%), and 2/100 or worse in three patients (27%) who developed postoperative glaucoma.
• CONCLUSION: Despite microcorneas, favorable visual outcomes were achieved after early surgery in this series. However, adequate management of postoperative complications, especially glaucoma, is required. (Am J Ophthalmol 2007;144:276–280. © 2007 by Elsevier Inc. All rights reserved.)

PROGRESS IN EARLY SURGERY HAS IMPROVED THE visual prognosis of congenital cataracts, and excellent visual acuities and stereopsis can be obtained in cases of bilateral cataracts. However, congenital cataract with a microcornea has a relatively poor prognosis attributable to associated ocular and systemic anomalies and the high rate of severe postoperative complications, including glaucoma, corneal opacity, and secondary membrane formation.[1–7] Early surgery for congenital cataracts in the presence of a microcornea is technically difficult because of the small hazy cornea, shallow anterior chamber, poor pupil dilation, and persistent tunica vasculosa lentis, and few reports have focused specifically on the surgical results in these eyes.[1] Several reports have suggested that early surgery for congenital cataract is a risk factor for postoperative complications including glaucoma.[8–10] The long-term prognosis and the most favorable time for performing cataract surgery remain unclear, especially for eyes with microcornea. We retrospectively evaluated the surgical outcomes of patients who underwent early surgery within 12 weeks of age for bilateral congenital cataracts associated with microcornea.

Accepted for publication Apr 9, 2007.

From the Department of Ophthalmology, National Center for Child Health and Development, Tokyo, Japan (S.N., E.N., N.A.); and Kyorin Eye Center, Kyorin University School of Medicine, Tokyo, Japan (E.N.).
Inquiries to Sachiko Nishina, Department of Ophthalmology, National Center for Child Health and Development, 2-10-1 Ohkura, Setagaya-ku, Tokyo, 157-8535, Japan; e-mail: nishina-s@ncchd.go.jp

METHODS

• PATIENTS: We retrospectively reviewed the records of 22 eyes of 11 patients (seven boys and four girls) who underwent surgery for bilateral congenital cataracts with microcornea within 12 weeks of age at the National Center for Child Health and Development, Tokyo, Japan, between 1990 and 2003. The corneal diameters at the time of surgery ranged from 7.0 to 9.0 mm.

• SURGICAL PROCEDURES: All patients underwent lensectomy and anterior vitrectomy via the limbal approach using a 20-gauge surgical system (MVS XII or Accurus Surgical System; Alcon, Tokyo, Japan). A 25-gauge surgical system was used with one patient (Patient 11) who had extreme microcorneas. The mean patient age at surgery was 7.7 ± 3.3 weeks (range, two to 12 weeks). Aphakic eyes were corrected with spectacles or contact lenses postoperatively.

• EYE EXAMINATIONS: Visual acuities and the development of postoperative complications were evaluated every two to three months. If amblyopia was detected during follow-up, part-time occlusion therapy was applied. The best-corrected visual acuity was measured with a standard Japanese visual acuity chart using Landolt rings or pictures at 5 m, and then converted to Snellen visual acuity. Intraocular pressure (IOP) was measured with the use of Goldmann applanation tonometry (Möller-Wedel GmbH, Wedel, Germany). During infancy and young age, the IOP

0002-9394/07/$32.00
doi:10.1016/j.ajo.2007.04.019

TABLE 1. Preoperative Data and Outcome of Patients with Microcornea Undergoing Early Surgery for Bilateral Congenital Cataracts

Patient No.	Gender	Age at Surgery (weeks)	Corneal Diameter (mm) (OD, OS)	Type of Cataract (OU)	Associated Ocular/Systemic Anomalies	Postoperative Complications	Visual Acuity (OD, OS)	Visual Acuity (OU)	Follow-up (mos)
1	M	4	8.0, 7.5	Nuclear	Retinal degeneration (OS)/cystic kidney	Glaucoma, retinal hole (OS)	20/40, 2/100	20/40	199
2	F	12	9.0, 9.0	Nuclear			20/40, 20/25	20/20	183
3	F	2	8.0, 8.0	Membranous	PFV, pupillary occlusion (OS), retinal dystrophy (OU)/Smith-Lemli-Opitz syndrome	Glaucoma, corneal opacity (OU), rhegmatogenous RD (OS)	LP (+), LP (−)	LP (+)	174
4	M	8	8.5, 8.5	Nuclear		Glaucoma (OU), secondary membrane (OS)	20/25, 20/200	20/25	168
5	M	8	8.0, 8.0	Complete			20/100, 20/200	20/100	120
6	M	12	8.0, 8.0	Nuclear			20/200, 20/40	20/30	103
7	M	6	8.0, 8.0	Nuclear	Iris hypoplasia (OU)		20/50, 20/30	20/20	87
8	F	5	8.0, 8.0	Complete	Iris hypoplasia, tunica vasculosa lentis (OU)	Glaucoma, corneal opacity (OU)	LP (+), LP (+)	LP (+)	78
9	M	7	8.0, 8.0	Nuclear	Iris hypoplasia (OU)/developmental delay	Glaucoma, corneal opacity (OU)	1/100, 2/100	2/100	69
10	F	11	9.0, 9.0	Complete	Iris hypoplasia (OU)		20/25, 20/30	20/25	44
11	M	10	7.0, 8.0	Complete	Iris hypoplasia, retinal fold (OU)/Hallermann-Streiff syndrome	Exudative RD (OU)	2/100, 20/200	20/200	40

F = female; M = male; OD = right eye; OS = left eye; OU = both eyes; PFV = persistent fetal vasculature; RD = retinal detachment; LP = light perception.

TABLE 2. Aphakic Glaucoma after Early Surgery in Eyes with Bilateral Congenital Cataracts with Microcornea

Patient No.	Gender	Eye	Age at Surgery (weeks)	Corneal Diameter (mm)	Type of Cataract	Associated Ocular Anomalies	Postoperative Time at Onset of Glaucoma (mos)	Treatment	Visual Acuity
1	M	OS	4	7.5	Nuclear	Retinal degeneration	53	Medication + trabeculotomy	2/100
3	F	OD	2	8.0	Membranous	Retinal dystrophy	1	Medication	LP (+)
		OS	2	8.0	Membranous	PFV, pupillary occlusion, retinal dystrophy	1	Medication	LP (−)
4	M	OD	8	8.5	Nuclear		100	Medication	20/25
		OS	8	8.5	Nuclear		68	Medication + trabeculotomy	20/200
8	F	OD	5	8.0	Complete	Iris hypoplasia, tunica vasculosa lentis	2	Medication	LP (+)
		OS	5	8.0	Complete	Iris hypoplasia, tunica vasculosa lentis	2	Medication + trabeculotomy	LP (+)
9	M	OD	7	8.0	Nuclear	Iris hypoplasia	14	Medication	1/100
		OS	7	8.0	Nuclear	Iris hypoplasia	5	Medication + trabeculotomy	2/100

M = male; F = female; OD = right eye; OS = left eye; PFV = persistent fetal vasculature; LP = light perception.

TABLE 3. Characteristics of Eyes With and Without Aphakic Glaucoma After Early Surgery for Bilateral Congenital Cataracts With Microcornea

Parameter	Eyes with Postoperative Glaucoma n = 9		Eyes without Postoperative Glaucoma n = 13	
Age at cataract surgery (weeks)	2–8 (mean, 5.3)*		4–12 (mean, 9.4)	
Corneal diameter (mm)	7.5–8.5 (mean, 8.1)		7.0–9.0 (mean, 8.2)	
Type of cataract	Nuclear 5, complete 2, membranous 2		Nuclear 7, complete 6	
Associated ocular anomalies	Iris hypoplasia	4	Iris hypoplasia	6
	PFV, tunica vasculosa lentis	3	PFV, tunica vasculosa lentis	0
	Retinal dystrophy, degeneration	3	Retinal fold	2
Visual acuity	20/50–20/25	1	20/50–20/25	9
	20/200–20/100	1	20/200–20/100	3
	LP–2/100	7	LP–2/100	1

PFV = persistent fetal vasculature; LP = light perception.
*P = .0014 (Welch t test).

was measured using a Perkins hand-held applanation tonometer with the patient under general anesthesia. Glaucoma was defined as an IOP exceeding 21 mm Hg and increased cupping of the optic nerve head. The mean follow-up period was 115 ± 58 months (range, 40 to 199 months).

RESULTS

THE PREOPERATIVE CHARACTERISTICS AND POSTOPERATIVE results for all patients are shown in Table 1. The corneal diameter at the time of surgery was 9.0 mm in four eyes, 8.5 mm in two eyes, 8.0 mm in 14 eyes, and 7.5 mm or smaller in two eyes. The minimum corneal diameter was 7.0 mm. The morphologic types of cataract were nuclear in 12 eyes, complete in eight eyes, and membranous cataracts in two eyes. No patient had a morphologic difference in the type of cataract between the eyes. Fundus features could not be visualized by indirect ophthalmoscopy in any eye owing to the dense lens opacity.

Other preoperative ocular abnormalities included iris hypoplasia in 10 eyes and persistent tunica vasculosa lentis in three eyes. Persistent fetal vasculature (PFV) in the anterior segment including tunica vasculosa lentis caused pupillary occlusion in one eye. Pupil dilation using mydriasis was incomplete in all eyes. Seven eyes required pupilloplasty to perform lensectomy in periphery. Preoperative ultrasonography failed to detect any posterior segment anomalies; however, one patient had bilateral retinal dystrophy postoperatively, another patient had bilateral small retinal folds between the disk and fovea, and one eye of another patient had peripheral retinal degeneration. Systemic abnormalities were found in four patients (36%), including the Smith-Lemli-Opitz syndrome, Hallermann-Streiff syndrome, developmental delay, and cystic kidney.

Intraoperative complications did not occur in any eyes, while postoperative complications occurred in 11 eyes (50%) of six patients. The complication that occurred most frequently was glaucoma, which developed in nine eyes (41%). Table 2 shows the data from patients with postoperative aphakic glaucoma. Table 3 shows the features of eyes with and without glaucoma. All nine eyes with glaucoma underwent cataract surgery within eight weeks after birth. Thus, the incidence of the postoperative glaucoma in the 14 eyes in which cataract surgery was performed within eight weeks was higher (64%) than the overall (41%). Table 3 shows a significant difference in age at cataract surgery between eyes that developed glaucoma and eyes that did not (Welch t test, P = .0014). The corneal diameters at the time of cataract surgery in the nine eyes in which glaucoma developed ranged from 7.5 to 8.5 mm. Glaucoma did not develop in eyes with a corneal diameter of 9.0 mm in this series. Seven (78%) of the nine eyes with aphakic glaucoma had associated ocular anomalies besides microcorneas, including iris hypoplasia, PFV, and retinal dystrophy. All eyes had open angles, except for partial peripheral synechia at the incision site of cataract surgery by gonioscopy. The period between cataract surgery and the onset of glaucoma varied from one month to eight years. Four (44%) eyes of two patients (Patients 3 and 8) developed glaucoma within two months after cataract surgery; severe corneal opacity and deep amblyopia developed that resulted in poor visual prognosis. Persistent fetal vasculature was present in three of these four eyes. Glaucoma was controlled with medication alone in five (56%) eyes, while four (44%) eyes required trabeculotomy. At the final examination, the IOP was well controlled in all eyes; however, corneal opacity remained in six eyes (67%) of three patients (Patients 3, 8, and 9).

Other postoperative complications included exudative retinal detachment in two eyes (9%) of one patient, and a secondary membrane formation, a rhegmatogenous retinal detachment, and a retinal hole in one eye each (4.5%). An exudative retinal detachment developed five months after